Advances in Communication Technology, Computing and Engineering
***Editors*:** Mariyam Ouaissa, Mariya Ouaissa, Sarah El Himer, Zakaria Boulouard
pp. 68 – 78, Copyright © 2021 RGN Publications

Performance Analysis of Pioneer Single Baseline Phase Unwrapping Techniques

Tarek Bentahar[1], Atef Bentahar[2], and Riad Saidi[3]

[1]*LABGET-laboratory, Larbi Tebessi University, Tebessa, Algeria (tarek.bentahar@univ-tebessa.dz)*
[2]*LAMIS-laboratory, Larbi Tebessi University, Tebessa, Algeria (atef.bentahar@univ-tebessa.dz)*
[3]*LABGET-laboratory, Larbi Tebessi University, Tebessa, Algeria (riad.saidi@univ-tebessa.dz)*

Abstract. Phase unwrapping is a key step in the interferogram processing chain. This process reconstructs the phase images to obtain a 3D presentation of the scanned surface called digital elevation model. From 80's to date, several phase unwrapping algorithms have been proposed whose performance differs from one algorithm to another. Some algorithms are fast or accurate and there are other approaches that try to attain a tradeoff between accuracy and processing time. This paper analyzes the performance of some pioneering methods in the phase unwrapping field. The chosen methods are implemented and tested for real inSAR data provided by ESA ERS-1, and compared according to several relevant criteria to assess the computation time and accuracy of each one.

Keywords and phrases: inSAR interferogram; phase unwrapping; branch-cut; quality-guided; minimum- norm methods.

1 Introduction

The interferometric synthetic aperture radar (InSAR) system is a powerful and reliable remote sensing tool for studying the earth's surface. Its usefulness lies in its ability to operate day and night and in all weather conditions without being hampered by the presence of fog or cloud. InSAR is mainly employed in surface imaging to obtain topographic maps and digital terrain models (DEM) [1] or to detect surface changes [2]. The difference between SAR and inSAR is the double acquisition of the backscattered signal either by two antennas and one pass or one antenna and two passes [3]. The double acquisition of the signal makes the phase image more useful since the resulting interferogram only contains the phase related to the path traveled.

However, the inSAR interferogram is not directly usable because the phase values are wrapped into (-π, π] depending on the ambiguity altitude. To retrieve the true value of the phase which correctly interprets the attitude of the imaged point, the phase unwrapping process must be performed. Without residues (noise), the phase unwrapping is just a simple integration of the wrapped gradients into a two-dimensional grid. Unfortunately, there is no noise-free interferometric measurement. Indeed, interferograms are subject to many noises producing phase jumps called residues. The presence of these residues makes the use of the gradient integration alone not practical, because the error generated by the phase jumps propagates along the integration path forming distorted lines in the unwrapped image. To avoid the error propagation problem, several residue-immune phase unwrapping algorithms have been proposed [4-6].

Depending on the baseline and wavelength used, phase unwrapping can be categorized into three categories: single baseline (SB), multi baseline (MB), and large scale phase unwrapping (LS). In SB only one baseline and one wavelength are used, this is the most simple and practical type of interferometric measurement. Phase unwrapping in SB can be divided into three groups: path following, optimization-based, and filtering & unwrapping techniques [5]. The path following methods are also divided into two sub-groups: branch-cut (BC) and quality-guided (QG). And optimization methods into: minimum-norm (MN) and statistics-based methods.

BC methods [7-15] attempt to avoid residues entirely by establishing branches that connect these residues. Then, the basic unwrapping process is performed by avoiding all established branches. QG methods [16-24] rely on a quality map to guide the unwrapping process only in the good quality pixels or to guide the design of the mask that covers the bad pixels. MN methods [25-30] follow a completely different strategy, they treat the unwrapping problem with a global aspect not a local one like the case of the path-following methods. The global processing consists in finding an unwrapping solution using objective functions which minimizes the gradient difference between the supposed true unwrapped phase and the estimated one.

The computation time and the accuracy are the main competing points for unwrapping algorithms. Some methods are fast, others accurate, and others provide a compromise. However, the accepted perspective is that accuracy is usually at the expense of time. In this paper, a performance analysis of the pioneer methods is proposed in order to offer the strengths of each algorithm. The rest of the paper is organized as following: section 2 is devoted to explain the entity of the interferogram residue and the work principle of the phase unwrapping techniques. Section 3 depicts the performance analysis and discussion of the obtained results. Section 4 concludes the paper by revealing the difference points of each algorithm studied.

2 What is phase unwrapping?

All the phases of an interferogram are wrapped into the interval (–π, π] according to the equation (1), which gives the interferograms the fringe features with a local orientation and frequency proportional to the slope of the imaged cell.

$$\phi^{w} = \mathrm{Mod}_{2\pi}(\phi^{r} + \pi)\text{-}\pi \quad (1)$$

Where $\mathrm{Mod}_{2\pi}$ is the modulus function, ϕ^{w} and ϕ^{r} are the wrapped and the real phase respectively.

Due to shadow regions, inversion regions or system acquisition error some phases can be poorly measured which creates phase jumps in the grid. These jumps are the main source of residues in the interferogram. To detect residues, the sum of the wrapped gradients of the wrapped phase differences in 2x2 loop must be calculated using equation (2).

$$\begin{cases} R = \frac{1}{2\pi}\sum\left(\left(\Delta_{up}\right)^{w} + \left(\Delta_{down}\right)^{w} + \left(\Delta_{left}\right)^{w} + \left(\Delta_{right}\right)^{w}\right) \\ \Delta_{up} = \phi^{w}_{i+1,j} - \phi^{w}_{i,j} \\ \Delta_{down} = \phi^{w}_{i+1,j+1} - \phi^{w}_{i+1,j} \\ \Delta_{left} = \phi^{w}_{i,j+1} - \phi^{w}_{i+1,j+1} \\ \Delta_{right} = \phi^{w}_{i,j} - \phi^{w}_{i,j+1} \end{cases} \quad (2)$$

Where Δ is the gradient operation and indexes i, j are the row and column of the top-left pixel in the loop. According to (2) the pixels of the residue map have three values 0, +1 or –1, 0 for the healthy pixels, +1 or –1 are positive or negative residue respectively. The phase unwrapping consists of finding the real phase value from the wrapped one using equation (3). It is quite clear that from any unwrapped pixel we can unwrap its neighbor. But if a residue pixel is encountered the calculated phase will be erroneous and this error will propagate while calculating the following phases. The effect of error propagation results in distorted lines in the unwrapped image along the chosen path. So using (3) without considering any path choice process is not efficient with the presence of residues.

$$\phi^{u}_{i,j} = \phi^{u}_{n(i,j)} + \left(\phi^{w}_{i,j} - \phi^{w}_{n(i,j)}\right)^{w} \quad (3)$$

Where $\phi^{u}_{i,j}$ is the unwrapped phase of the current pixel (i,j) and $\phi^{u}_{n(i,j)}$is the neighboring unwrapped pixel.

To avoid error propagation, the basic phase unwrapping should not pass through a residue; this is the main purpose of the path-following methods with its two types BC and QG. BC methods aim to establish branches that connect the balanced residues with minimum total length. Therefore, the high residue density regions form a single cluster inaccessible for unwrapping process called void areas. The first algorithm of this category is called branch-cut of Goldstein [7]. Goldstein's algorithm describes a window-based residue connection mechanism starting with the dimension of 3x3 and growing until it connects all the residues. Residues remaining unbalanced can be connected to the edge in order to obtain a minimum length. In [8] the authors proposed to use the spanning tree algorithm to connect these residues. Still in order to have a minimum length, in [9] the authors proposed to use the finite element method after Goldstein's algorithm to optimize the connections obtained. In [10] the pseudo-correlation quality map was chosen for the same purpose. In [11] the authors adopted a global connection process using two

tables of the aggregated coordinates of positive and negative residues rather than a local process based on an increasing window. An approach almost similar to [11] has been proposed in [12] which is a global process based on a stochastic exchange and search operation. To minimize processing time, other enhancements have been proposed such as the spanning tree [13], B-Spline surface fitting [14], and Dynamic Adjacent Table [15].

QG methods adopt processes guided by a quality map, they are also a pixel by pixel processing of the path- following category. Guidance based on the quality map is used either to design a mask covering the bad pixels and then unwrap the good quality ones, or to directly guide the unwrapping only in the good quality pixels and avoid the bad ones. Flynn [16] was the first to propose the use of a quality map with the region growing technique to mask the poor quality pixels, then the basic process is performed by avoiding the designed masks. Another algorithm similar to that of Flynn has been proposed in [17] but in an upside down concept i.e. determining the good quality pixels by the region growing technique which will be unwrapped. Herráez [18] proposed a reliable algorithm based on sorting the quality of the pixel edges, then unwrap the pixels according to the edge quality priority. Zhong et al. [20] used a statistics table called Priority Queue and a new Max gradient-based quality map to unwrap all pixels in the interferogram. In [21] a further improvement of the Herráez algorithm was proposed, it employs the same sorting described in [18] based on the quality map and the residue mask map. In [22] a double phase unwrapping method has been proposed: first with the ordinary algorithm guided by the quality, then the resulting unwrapped image is divided into two levels: high and low quality. In low quality areas, the process of minimizing discontinuity is performed to eliminate all gaps. In [23] the authors presented a new quality map based on a combination of distance to residues and ordinary quality map. In [24] another improvement in the quality-guided phase unwrapping has been proposed. The proposed improvement uses a new quality weighted map where weights are calculated from the map of residues in a modified range for the azimuthal and distal directions.

Optimization methods have a totally different strategy than the path-following. These methods try to minimize the difference between the unwrapped image estimated by the basic process and the found one. In optimization methods a predefined objective function has to be used as it is shown in the general model of equation (4).

$$\arg\min \sum_{.} f[(\phi^{u}{}_{i,j} - \phi^{u}{}_{n(i,j)}) - (\phi^{w}{}_{i,j} - \phi^{w}{}_{n(i,j)})] \tag{4}$$

Where *f(.)* is the generalized objective function. If *f(.)* = $|.|^{p}$, in this case we are in minimum-norm L^{p} space [26]. Therefore many classes can be considered according to P such as L^{2}[25,27] and L^{1} [28-30], and also in filtering applications [31-32].

Flynn's minimum discontinuities method [28] is based on the idea of limiting phase discontinuities only in noisy areas. This leads to use a minimization procedure of a weighted

sum between the noisy areas and the noise-free ones. The Flynn's algorithm consists in dividing the unwrapped image into two connected regions, and then one of these regions is adjusted by a cycle multiple using the weighted sum minimization. This process should be repeated until no two regions exist in the resulted wrapped image. A reliable improvement of Flynn's algorithm is proposed in [30], it aims to overcome the shortcoming of Flynn's method which is time-consuming. The method is called pre-unwrapping-assisted minimum discontinuities, which is fast and has near same quality as unwrapped phase image using Flynn's method.

Minimum Cost flow (MCF) method of Costantini [29] is based on the fact that any neighboring phase differences can be estimated by a substantial gap of 2π multiple. This leads to consider the minimization problem depends only on integer variables.

The first L^2 norm phase unwrapping method was proposed by Ghiglia and Romero [25]. As the objective function is $\|.\|^2$, their method is of the least square type. The method is based on weighted and unweighted least-squares minimization, obtained by the discrete cosine transform. In [27] other weighted least square algorithm is proposed. The method belonging to the multigrid techniques solves the equations on smaller and coarser grids using Gauss-Seidel minimization model.

3 Results and Discussions

In this section the performance of Glodstein's branch-cut (BC) [7], Ghiglia's quality-guided (QG) [4], Herráez QG [18], Ghiglia's minimum-norm (MN) [25], and costantini's minimum cost flow (MFC) [29] algorithms are analyzed and discussed in two main performance criteria: time and accuracy. The obtained results; especially for the computation time evaluation, depend on the hardware material used for our implementation which is: intel CPU-I5 2.5 GHz and 8 Gbytes RAM. The accuracy is evaluated according to three main metrics suitable to the real interferogram data test where the referential image is not available. The used metrics are: Average gradient (AG), Discontinuity Point Index (DPI) and Itoh condition-based phase unwrapping error (IPUE). The inSAR interferogram chosen for the test is provided by ESA ERS-1 of Vatnajökull region. The cropped size is 200x200 pixels with 0.0112 % residues rate. This interferogram (refer to figure 1a) has no-uniform residues distribution and contains different fringe frequencies, it can be regarded as a credible test data for the five above said methods. Figures 1b, c, d, e, and f shows the resulted unwrapped phase image using Glodstein's BC, Ghiglia's QG, Herráez QG, Ghiglia's MN, and Costantini's MFC methods respectively.

For a visual qualitative analysis, the overall quality of the minimum norm methods is satisfactory compared to other categories of path-following techniques. Indeed, we can see that unwrapped images of figures (1e and f) contain fewer discontinuities i.e. pixel color graduation is homogenous and there are less abrupt variations. However, due to the global minimization process used in minimum-norm techniques, some high residues density areas are over-smoothed. Therefore, some local details including the original sharp edges can be lost. Comparing the path-

following techniques, the quality of QG techniques is better than BC in terms of edge variations especially in noisy areas. Indeed, using Glodstein's BC algorithm, high residues density regions are completely avoided and remain no-unwrapped which explains the isolated regions of high edge variation in figures 1b. Whereas, using the quality-guided methods, these same regions are better unwrapped and they are not excessively smoothed as with minmum-norm techniques.

The obtained gradient images (figure 2) of the wrapped each unwrapped image shown in figure 1 can give a glimpse on the occurred discontinuities and the isolated regions. Of course, the wrapped image (interferogram) is the most discontinuous (refer to figure 2a) due to the noisy areas and mainly due to the fringe lines of modulo 2π operation. In figures 2b, c, d, e, and f, there are no fringe lines and the discontinuities are only in the noisy areas depending on the residues density. Figure 3 shows the residues map of the interferogram used, we can see that the residues density is not uniform and there is a coherent link between these residues and the discontinuities resulted in each unwrapped image.

For a quantitative analysis, the obtained results using the above cited metrics are indicated in table 1. The obtained computation time shows that Goldstein's method is the fastest. Indeed, the next technique which is Gighlia's QG algorithm is approximately seven times slower. Minimum-norm methods consume more computing time, approximately 19 and 15 seconds for Gighlia's MN and Costantini's MCF respectively. Regarding the obtained accuracy under AG, DPI and IPUE metrics, the results show that Goldstein's algorithm is not accurate enough compared to other algorithms. This leak is due to the isolated regions of high residues density.

Both minimum-norm methods present a good accuracy in terms of discontinuities occurred in the unwrapped image. Indeed, their accuracy metrics are lower than those of the three path-following algorithms. As a comparison between minimum-norm techniques, L1 norm presented by Costantini's MCF algorithm is more accurate than L2 norm (Ghiglia's MN), but at the expense of the computation time. For the quality-guided methods, the obtained results show that they present a satisfactory compromise between the two criteria.

	Goldstein's BC	Gighlia's QG	Herráez's QG	Ghiglia's MN	Costantini's MCF
Computation Time (sec)	1.4013	10.5467	14.5048	15.6512	18.9851
Normalized Time	1	7.5263	10.5309	11.1690	13.5482
AG (rad)	0.3826	0.3511	0.3493	0.2768	0.1849
DPI(%)	0.1281	0.0824	0.0896	0.0895	0.0744
IPUE(%)	0.8375	0.8386	0.8325	0.5768	0.3245

Table 1: Results in terms of computation time, AG, DPI and IPUE

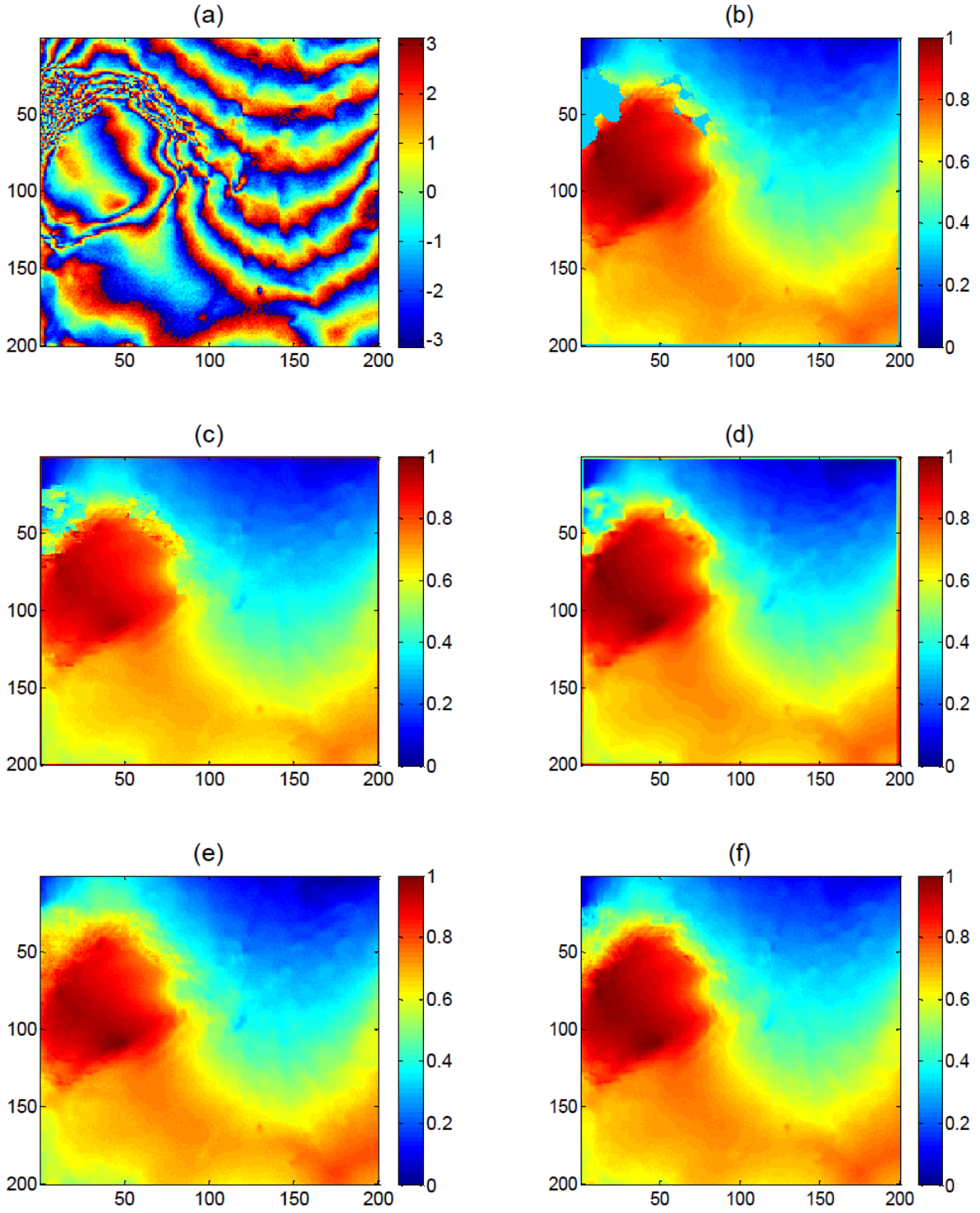

Figure 1: (a) real interferogram, (b) wrapped image using Goldstein's method, (c) Ghiglia's QG method, (d) Herráez method; (e) Ghiglia's MN method and (f) Costantini's method.

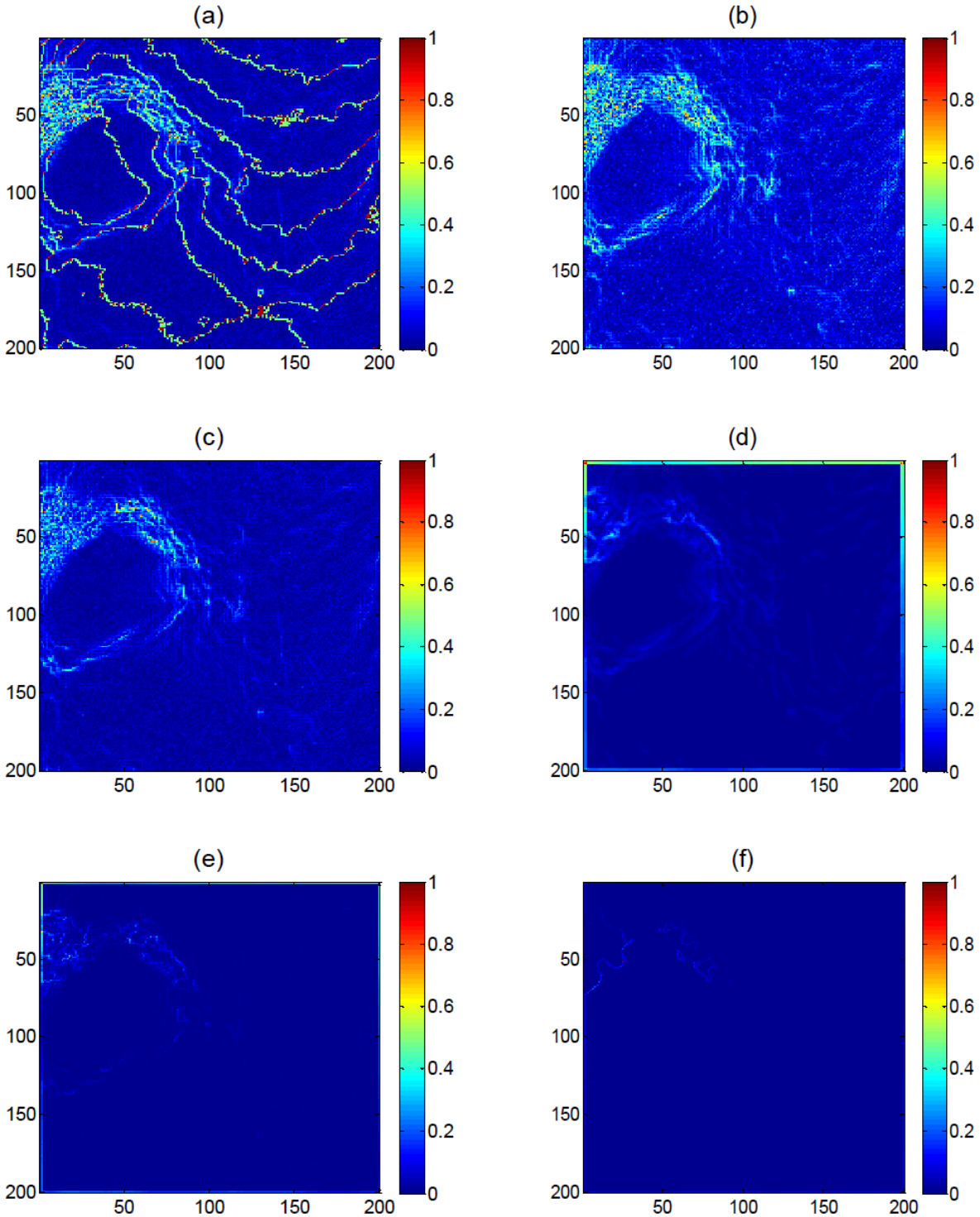

Figure 2: Normalized gradient image of: (a) real interferogram, (b) wrapped image using Goldstein's method, (c) Ghiglia's QG method, (d) Herráez method; (e) Ghiglia's MN method and (f) Costantini's method.

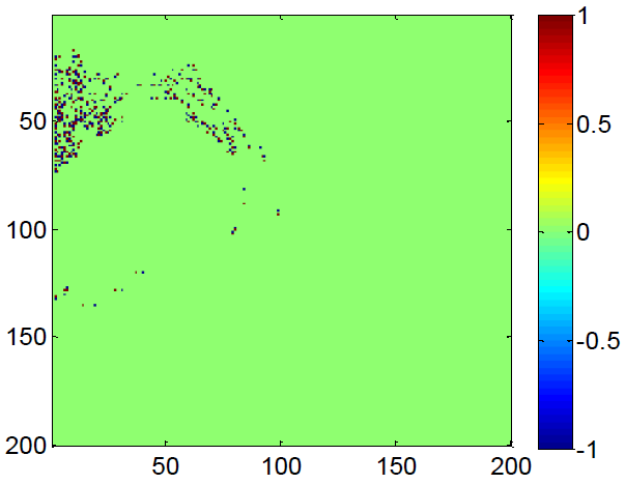

Figure 3: Residues map of the real interferogram

4 Conclusion

In this paper a comparative analysis of five phase unwrapping pioneer algorithms for inSAR interferogram processing is presented. This analysis aims to reveal the main substantial differences of the studied algorithms in terms of computation time and accuracy. In order to construct a more practical analysis, the chosen methods belong to different classes and categories, and the test was carried out for no-uniform real interferogram. Computation time, AG, DPI, and IPUE are used as metrics to evaluate the performance of each method. The obtained results show that Goldstein's branch-cut method is very fast, and the skillful minimum methods are time consumer. However, in term of accuracy, minimum norm methods are more accurate and provide fewer discontinuities in the resulted wrapped image. As a tradeoff between time and accuracy, the quality-guided methods present a good compromise. Through this study, algorithmic development such as hybridization between two or more pioneer techniques can end up to efficient and reliable methods. These hybrid methods may provide an optimized tradeoff between time and accuracy.

Acknowledgement

Authors would like to express thanks to LABGET members for their help and contributions, to DGRST for the useful platform SNDL, to ESA for providing ERS-1 inSAR data.

References

[1] H A. Geymen, Digital elevation model (DEM) generation using the SAR interferometry technique, Arabian Journal of Geosciences 7 (2012), 827–837. DOI: 10.1007/s12517-012-0811-3.

[2] O. Monserrat , M. Crosetto and G. Luzi, A review of ground-based SAR interferometry for deformation measurement, Journal of Photogrammetry and Remote Sensing, 93 (2014), 40–48, DOI: 10.1016/j.isprsjprs.2014.04.001.
[3] A. Moreira, P. Prats-Iraola, M.Younis, G. Krieger, I. Hajnsek and K. P. Papathanassiou, A tutorial on synthetic aperture radar. IEEE Geoscience and Remote Sensing Magazine, 1 (2013), 6–43. DOI: mgrs.2013.2248301.
[4] D. C. Ghiglia and M. D. Pritt, Two-Dimensional Phase Unwrapping: Theory, Algorithms, and Software, New York-Wiley (1998). ISBN: 978-0-471-24935-1.
[5] H. Yu, Y. Lan, Z. Yuan, J. Xu, and H. Lee, Phase Unwrapping in InSAR : A Review, IEEE Geoscience and Remote Sensing Magazine, 7 (2019), 40–58, DOI: 10.1109/mgrs.2018.2873644.
[6] R. Gens, Two-dimensional phase unwrapping for radar interferometry: Developments and new challenges, International Journal of Remote Sensing, 24 (2003), 703–710. DOI: 10.1080/0143116021000016725.
[7] R. M. Goldstein, H. A. Zebker and C. L. Werner, Satellite radar interferometry: Two dimensional phase unwrapping, Radio Science, 23 (1988), 713–720, DOI: 10.1029/rs023i004p00713.
[8] N. H. Ching, D. Rosenfeld and M. Braun, Two-dimensional phase unwrapping using a minimum spanning tree algorithm, IEEE Transactions on Image Processing, 1 (1992), 355–365. doi.org/10.1109/83.148608.
[9] W. Nan and F. Dazheng, InSAR phase unwrapping algorithm using the brahch-cut and finite element method, Proceedings 7th International Conference on Signal Processing, (2004), DOI: 10.1109/icosp.2004.1442151.
[10] X. Feng, W. Jicang, Z. Lei and L. Xiaoling, A new method about placement of the branch cut in two-dimensional phase unwrapping. Proceeding 1st Asian and Pacific Conference on Synthetic Aperture Radar, (2007), doi:10.1109/apsar.2007.4418721.
[11] C. Li and D.-Y. Zhu, A residue-pairing algorithm for inSAR phase unwrapping, Progress In Electromagnetics Research, 95 (2009), 341–354. DOI: 10.2528/pier09070706.
[12] D. Zheng and F. Da, A novel algorithm for branch cut phase unwrapping, Optics and Lasers in Engineering, 49 (2011)., 609–617. DOI: 10.1016/j.optlaseng.2011.01.017.
[13] H. Yu, M. Xing and Z. Bao, A Fast Phase Unwrapping Method for Large-Scale Interferograms, IEEE Transactions on Geoscience and Remote Sensing, 51 (2013), 4240–4248 DOI: 10.1109/tgrs.2012.2229284.
[14] Z. Yand X. ZiJian, A Phase Unwrapping Algorithm Based on Branch-cut and B-Spline Fitting in InSAR, 2018 IEEE International Conference on Signal Processing, Communications and Computing (2018), DOI:10.1109/icspcc.2018.8567735.
[15] T. Liu, Z. Shang, J. Wu, D. Zhou and S. Yan, Improved branch-cut phase unwrapping strategy based on dynamic adjacent table. The Journal of Engineering, 2019 (2019), 5805–5809, DOI: 10.1049/joe.2019.0352.
[16] T. J. Flynn, Consistent 2-D phase unwrapping guided by a quality map, International Geoscience and Remote Sensing Symposium (1996), DOI: 10.1109/igarss.1996.516887.
[17] X. Wei and I. Cumming, A region-growing algorithm for InSAR phase unwrapping, IEEE Transactions on Geoscience and Remote Sensing 37 (1999), 124–134, DOI:10.1109/36.739143.
[18] M. A. Herráez, D. R. Burton, M. J. Lalor and M. A. Gdeisat, Fast two-dimensional phase-unwrapping algorithm based on sorting by reliability following a noncontinuous path, Applied Optics 41 (2002), 7437–7444, DOI:10.1364/ao.41.007437.
[19] H. S. Abdul-Rahman, M. A. Gdeisat, D. R. Burton, M. J. Lalor, F. Lilley and C. J. Moore, Fast and robust three-dimensional best path phase unwrapping algorithm, Applied Optics 46 (2007), 6623–6635, DOI:10.1364/ao.46.006623.

[20] H. Zhong, J. Tang, S. Zhang and M. Chen, An Improved Quality-Guided Phase-Unwrapping Algorithm Based on Priority Queue, IEEE Geoscience and Remote Sensing Letters 8 (2011), 364–368. DOI: 10.1109/lgrs.2010.2076362.
[21] Z. Dai and X. Zha, An Accurate Phase Unwrapping Algorithm Based on Reliability Sorting and Residue Mask, IEEE Geoscience and Remote Sensing Letters 9 (2012), 219–223. DOI:10.1109/lgrs.2011.2165198.
[22] H. Zhong, J. Tang, S. Zhang, and X. Zhang, A Quality-Guided and Local Minimum Discontinuity Based Phase Unwrapping Algorithm for InSAR/InSAS Interferograms. IEEE Geoscience and Remote Sensing Letters 11 (2014), 215–219, DOI:10.1109/lgrs.2013.2252880.
[23] G. Jian, Reliability-Map-Guided Phase Unwrapping Method, IEEE Geoscience and Remote Sensing Letters 13 (2016), 716–720. DOI:10.1109/lgrs.2016.2539298.
[24] H. Wang, L. Tong, Y. Li and F. Xiao, Phase Unwrapping Algorithm Based on Improved Weighted Quality Graph, IEEE International Geoscience and Remote Sensing Symposium (2019), DOI:10.1109/igarss.2019.8898671.
[25] D. C. Ghiglia and L. A. Romero, Robust two-dimensional weighted and unweighted phase unwrapping that uses fast transforms and iterative methods, Journal of the Optical Society of America A 11 (1994), 107–117, DOI:10.1364/josaa.11.000107.
[26] D. C. Ghiglia and L. A. Romero, Minimum Lp-norm two-dimensional phase unwrapping. Journal of the Optical Society of America A 13 (1996), 1999–2013, DOI:10.1364/josaa.13.001999.
[27] M. D. Pritt, Phase unwrapping by means of multigrid techniques for interferometric SAR, IEEE Transactions on Geoscience and Remote Sensing 34 (1996), 728–738. DOI:10.1109/36.499752.
[28] T. J. Flynn, Two-dimensional phase unwrapping with minimum weighted discontinuity, Journal of the Optical Society of America A 14 (1997), 2692–2701, DOI:10.1364/josaa.14.002692.
[29] M. Costantini, A novel phase unwrapping method based on network programming, IEEE Transactions on Geoscience and Remote Sensing 36 (1998), 813–821, DOI:10.1109/36.673674.
[30] J. Xu, D. An, X. Huang and P. Yi, An Efficient Minimum-Discontinuity Phase-Unwrapping Method, IEEE Geoscience and Remote Sensing Letters, 13 (2016), 666–670. DOI:10.1109/lgrs.2016.2535159.
[31] Z. Suo, Z. Li and Z. Bao, A New Strategy to Estimate Local Fringe Frequencies for InSAR Phase Noise Reduction, IEEE Geoscience and Remote Sensing Letters 7 (2010), 771–775. DOI:10.1109/lgrs.2010.2047935.
[32] H. Yu, Y. Lan, H. Lee and N. Cao, 2-D Phase Unwrapping Using Minimum Infinity-Norm. IEEE Geoscience and Remote Sensing Letters 15 (2018), 1887–1891, DOI:10.1109/lgrs.2018.2865601.